 CMES, vol.11, no.3, pp.121-130, 2006

Analysis of Partially Concrete-Filled Steel Tubular Columns subjected to Cyclic Loadings

T. Ishizawa [1] **and M. Iura** [1]

Abstract: A one-dimensional model is proposed for numerical analysis of partially concrete-filled steel tubular (PCFST) columns subjected to cyclic loadings. The present formulation does not require experimental results nor shell analysis to obtain the constitutive equation of the model. The material properties and dimensions of PCFST columns are required for numerical analysis of the present model. The PCFST columns are assumed to consist of elastic beam and base plastic-hinge region in which steel local buckling is observed. Two parameters are introduced in order to express hardening phenomena of PCFST columns subjected to cyclic loading. Resisting forces due to concrete filled in the elastic beam are defined by using the present parameter. The other parameter is used to define an effective area of concrete filled in the base plastic-hinge region. The hysteretic rules for two parameters are proposed to model the hardening phenomena. For overall analysis, steel plates at the base plastic-hinge region are discretized along circumferential direction by using fiber elements, while layer elements are employed for concretes at the base plastic-hinge region. The validity of the present model has been confirmed through comparisons with existing experimental results.

keyword: Tubular columns, Concrete-filled columns, Inelastic response, Hysteretic model, Fiber model.

1 Introduction

The 1995 Kobe, Japan, earthquake caused widespread damage to steel bridge piers. A variety of methods have been proposed to strengthen the existing columns. Important issues for retrofitting the existing columns were strength and ductility. When the ultimate strength of steel tubular columns increases, massive substructures will be required. Since reinforcement of the existing substructures is expensive and time consuming, the increase of ultimate strength is not desirable. On the other hand, the increase of ductility in steel tubular columns is favorable for seismic design. Longitudinal stiffeners [Iura, Kumagai and Komaki (1997), The Public Works Research Institute, Metropolitan Expressway Public Corp., Hanshin Expressway Public Corp., Nagoya Expressway Public Corp., Kozai Club and Japan Association of Steel Bridge Construction (1997)], concrete infill [Iura, Orino and Ishizawa (2002), The Public Works Research Institute, Metropolitan Expressway Public Corp., Hanshin Expressway Public Corp., Nagoya Expressway Public Corp., Kozai Club and Japan Association of Steel Bridge Construction (1997), Usami and Ge (1994), Ge and Usami (1996)], carbon fiber sheets [Watanabe, Ishida, Hayashi, Yamaguchi and Ikeda (2002)] and patch plates [Chu and Sakurai (2004)] have been used to increase the ductility of steel tubular columns. From an economic and construction point of view, concrete infill would be one of the best choices for increasing ductility.

Concrete-filled steel tubular (CFST) columns have been used in many structural applications. When concrete is fully filled in steel bridge piers, the strength and ductility of CFST columns increase. However, the increases of ultimate strength and dead load require massive substructures. Especially when the existing structures are retrofitted, the increases of ultimate strength and dead load are unfavorable for substructures. Therefore, partially concrete-filled steel tubular (PCFST) columns have received wide attention in steel bridge piers. Amano, Kasai, Usami, Ge, Okamoto and Maeno (1998) have proposed an optimum concrete volume for rectangular PCFST columns. Ge and Usami (1996) have reported experimental results for rectangular cross-sections and shown that the attachment of a diaphragm on the top of concrete increases the ultimate strength and ductility of rectangular PCFST columns. Susantha, Ge and Usami (2002) have proposed a numerical model of rectangular CFST columns subjected to cyclic loading. According to Usami and Ge (1994), the filled-in concrete prevented steel plates from buckling inside columns. Therefore,

[1] Department of Civil and Environmental Engineering, Tokyo Denki University, Ishizaka, Hatoyama, Hiki, Saitama 350-0394, Japan

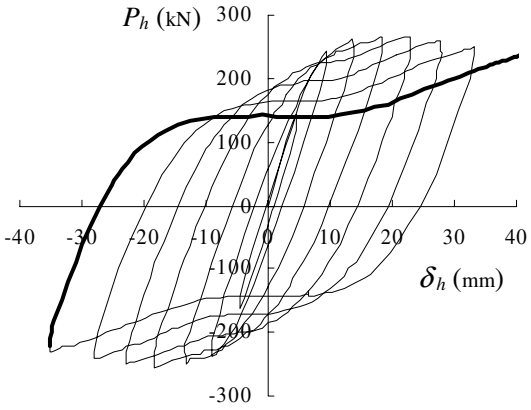

Figure 1 : Experimental result.

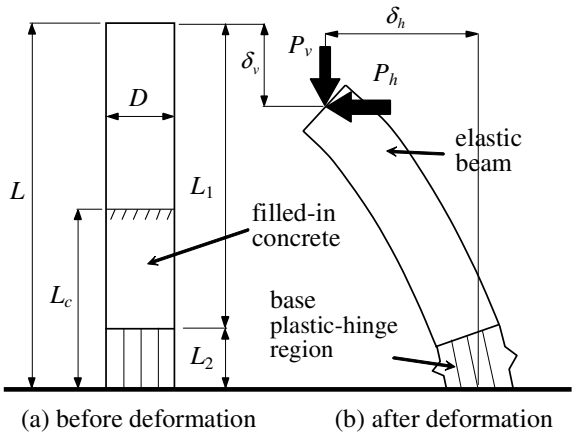

Figure 2 : Model of pier.

the ultimate strength of rectangular PCFST columns increases.

In comparison with works concerning rectangular PCFST columns, a small number of studies have been reported on circular ones. According to Iura, Kumagai and Komaki (1997), an elephant foot bulge was a typical local buckling mode of circular columns. In this case, steel plates deformed outside columns, so that the filled-in concrete did not prevent steel plates from buckling. Iura, Orino and Ishizawa (2002) have developed the formulae for evaluating ultimate strength and optimum concrete volume for circular PCFST columns. Morishita, Aoki and Suzuki (2000) and Iura, Orino and Ishizawa (2002) have shown that attachment of a diaphragm on the top of concrete increases ultimate strength and ductility of circular PCFST columns.

In this paper, a one-dimensional model is proposed for numerical analysis of circular PCFST columns. A finite element analysis is a powerful tool for analysis of PCFST columns. However, since finite element analysis is expensive for seismic design of steel bridge piers, a single degree of freedom model (e.g. Iura, Suetake and Atluri (2003)) is proposed to investigate the inelastic behavior of PCFST column. The critical issue for modeling the PCFST column subjected to cyclic loading is the hardening phenomena. A typical experimental result of PCFST column is shown in Fig. 1. A thick solid line denotes the hardening phenomena mentioned above.

In this model, PCFST column consists of two parts, as shown in Fig. 2. The lower part is called the base plastic-hinge region, while the upper part is called the elastic beam. The skeleton curves of steel plates and concretes at the elastic beam are assumed to be linear. We employ a constitutive equation of steel plate at the base plastic-hinge region, developed by Ishizawa and Iura (2005). The strength deterioration due to steel local buckling was taken into account in the constitutive equation. As concrete constitutive equation at the base plastic-hinge region, we employ a model developed by Susantha, Ge and Usami (2001).

The present analysis consists of two steps. In the first step, concretes in the elastic beam are neglected. Steel plates in the base plastic-hinge region are discretized along circumferential direction by using fiber elements, while concretes of the base plastic-hinge region are modeled by using layer elements, as shown in Fig. 3. We reduce a concrete area in the plastic-hinge region by introducing a parameter, since the constitutive equation of concretes used has been developed for confined concretes. The reduction of concrete area is motivated also by the fact that a separation and a slipping were observed between steel plates and concretes. The second step is to obtain a resisting force due to concretes in the elastic beam. For simplicity, we consider a concrete cantilever beam. Another parameter is introduced to calculate the resisting force. The introduction of two parameters is the key point for expressing the hardening phenomena of PCFST columns subjected to cyclic loadings.

Detailed comparisons between experimental and numerical results are made in this paper. The effects of concrete height and diaphragm on the behavior of PCFST columns are discussed.

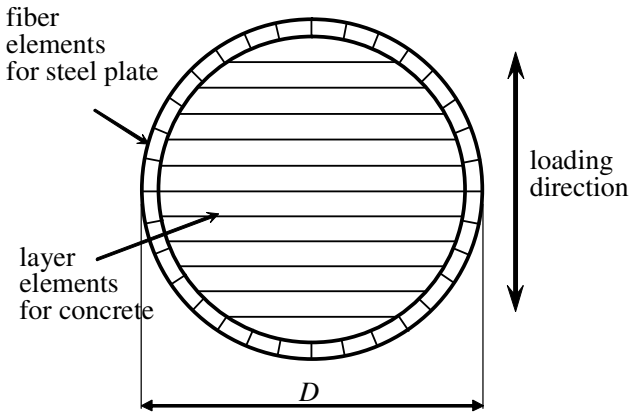

Figure 3 : Section model.

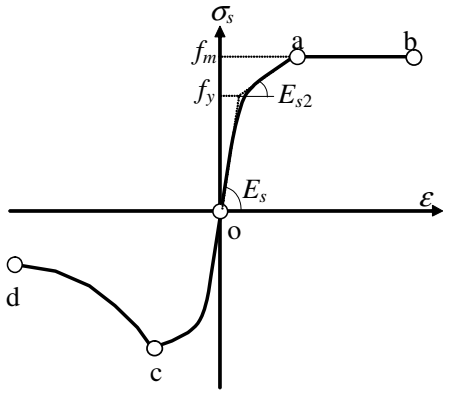

Figure 4 : Skeleton curve of stress-strain relation for steel at base plastic-hinge region.

2 One-dimensional model

We consider a circular PCFST column, as shown in Fig. 2, which is fixed at one end and subjected to axial load P_v and lateral load P_h at the other end. The axial load corresponds to the dead load of bridge girders, while the lateral load corresponds to the earthquake load. Notations L, L_c and D are the height of steel column, the height of filled-in concert and the outside diameter of steel column, respectively. As shown in Fig. 2(b), the PCFST column is assumed to consist of an elastic beam and a base plastic-hinge region. The height of base plastic-hinge region, denoted by L_2, was proposed by Ishizawa and Iura (2005) and given by

$$L_2 = 0.275\sqrt{\frac{I_0}{A_0}}\left\{\frac{D}{t}\frac{D}{L}\left(\frac{f_y}{E_s}\right)^{0.5} n_j^{-0.5}\right\}^{-0.596} \tag{1}$$

with

$$n_j = 1 - \frac{P_v}{A_0 f_y} \tag{2}$$

where I_0 and A_0 are the moment of inertia and cross-sectional area of steel column without filled-in concrete, t is thickness of steel plate, f_y and E_s are yield stress and Young's modulus of steel plate.

The skeleton curve of steel plate at the base plastic-hinge region, which has been proposed by Ishizawa and Iura (2005), is shown in Fig. 4. In the tensile side of skeleton curve, the maximum stress f_m, the yield stress f_y and Young's modulus E_s are obtained from a coupon test of steel materials. The slope of E_{s2} is determined by the geometrical and material data of steel plates. The smooth curve from o to a is obtained by using the modified Manegotto-Pinto model proposed by Sakai and Kawashima (2003). The compressive side of skeleton curve expresses the strength deterioration due to steel local inelastic buckling. Point c and deterioration curve from c to d are obtained by using the modified Shanley's model. The numerical model used is the same as that shown in Fig. 2, except for concretes. The smooth curve from o to c is obtained by using the modified Manegotto-Pinto model. The governing rules and the details of the constitutive equation for steel plate were given by Ishizawa and Iura (2005).

3 Concrete model

A variety of constitutive equations for concrete have been proposed. Recently Ferretti (2004) have developed a cell method for analysis of concrete cracking. We employ, herein, the constitutive equation of concrete proposed by Susantha, Ge and Usami (2001) and Susantha, Ge and Usami (2002). For completeness, at first, we briefly explain the constitutive equation for concrete.

3.1 Constitutive equation of filled-in concrete

In the concrete-filled steel tubular columns, the filled-in concrete is stronger than plain concrete due to confinement by steel column, and the slope of descending branch after peak stress is slow. Susantha, Ge and Usami (2001) have developed the stress and strain relationship of confined concrete, as shown in Fig. 5. The confined concrete

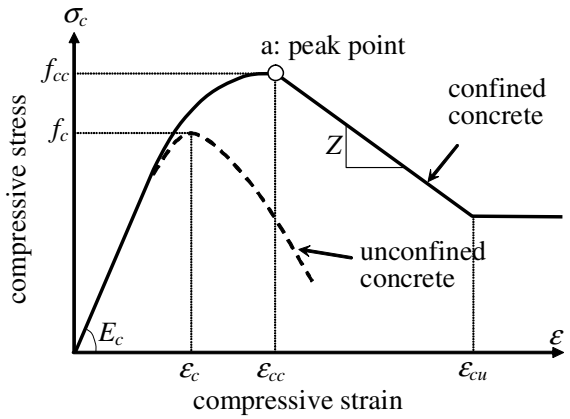

Figure 5 : Skeleton curves of stress-strain relations for confined and unconfined concrete.

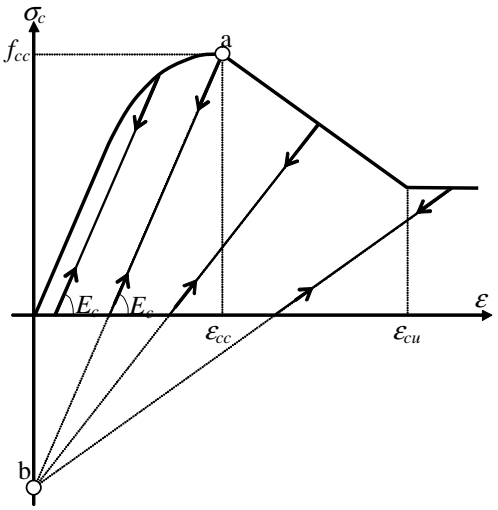

Figure 6 : Governing rules for confined concrete.

strength f_{cc} is given by

$$f_{cc} = 0.85 f_c + 4 f_{rp} \tag{3}$$

with

$$f_{rp} = \beta \frac{2t}{D-2t} f_y \tag{4}$$

where f_c is the unconfined concrete strength and f_{rp} is the maximum average lateral pressure on concrete. Parameter β is defined by

$$\beta = \upsilon_e - \upsilon_s \tag{5}$$

where υ_e and υ_s are the Poisson rations of a steel plate with and without filled-in concrete, respectively. Here υ_s is taken as equal to 0.50, and υ_e is given by the following expressions;

$$\upsilon_e = 0.2312 + 0.3582\upsilon'_e - 0.1524\left(\frac{f_c}{f_y}\right) + 4.843\upsilon'_e\left(\frac{f_c}{f_y}\right) - 9.169\left(\frac{f_c}{f_y}\right)^2 \tag{6}$$

$$\upsilon'_e = 0.881\times10^{-6}\left(\frac{D}{t}\right)^3 - 2.58\times10^{-4}\left(\frac{D}{t}\right)^2 + 1.953\times10^{-2}\left(\frac{D}{t}\right) + 0.4011 \tag{7}$$

Stress-strain relation up to the peak point is expressed as

$$\sigma_c = f_{cc}\frac{(\varepsilon/\varepsilon_{cc})r}{r-1+(\varepsilon/\varepsilon_{cc})^r} \tag{8}$$

where

$$r = \frac{E_c}{E_c - f_{cc}/\varepsilon_{cc}} \tag{9}$$

$$\varepsilon_{cc} = \varepsilon_c\left\{1+5\left(\frac{f_{cc}}{f_c}-1\right)\right\} \tag{10}$$

Notations σ_c and ε denote the longitudinal compressive stress and strain, respectively. Notation ε_c, which is the strain at maximum stress in unconfined concrete, is proposed by Tang, Hino, Kuroda and Ohta (1996) and given by

$$\varepsilon_c = \frac{20 f_c}{1.27\times10^5 + 4150 f_c} \tag{11}$$

The descending branch slope Z, appeared after a peak point as shown in Fig. 5, is given by

$$Z = \begin{cases} 0 & \left(\frac{R_t f_c}{f_y} \le 0.006\right) \\ \frac{10^5 R_t f_c}{f_y} - 600 & \left(\frac{R_t f_c}{f_y} \ge 0.006, f_y \le 283MPa\right) \\ \frac{10^6 R_t f_c}{f_y} - 6000 & \left(\frac{R_t f_c}{f_y} \ge 0.006, f_y \ge 336MPa\right) \\ \left(\frac{f_y}{283}\right)^{13.4}\frac{10^5 R_t f_c}{f_y} - 600 & \left(\frac{R_t f_c}{f_y} \ge 0.006, 283 \le f_y \le 336MPa\right) \end{cases} \tag{12}$$

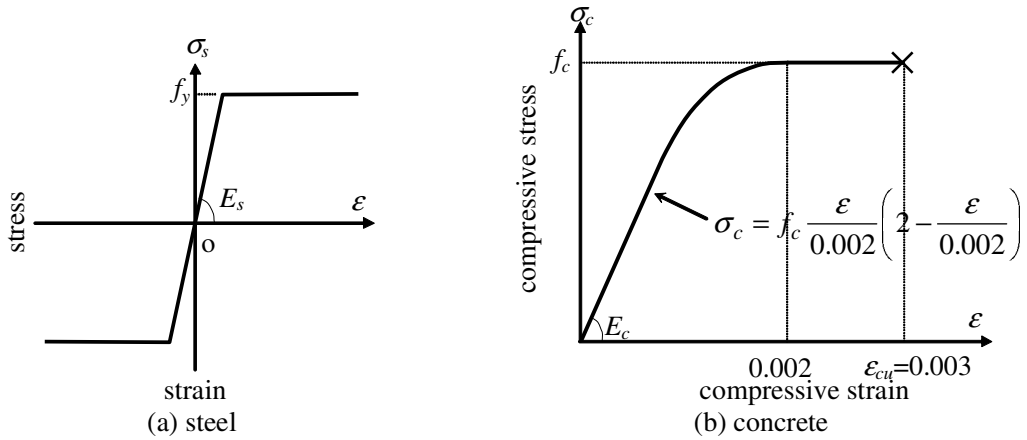

Figure 7 : Stress-strain relation of steel and concrete for the ultimate moment $M_{u(s+c)}$.

where

$$R_t = \sqrt{3(1-\upsilon^2)}\frac{f_y}{E_s}\frac{D}{2t} \tag{13}$$

where υ is the Poisson ratio of steel plate. Finally, the ultimate strain ε_{cu} is taken as 0.025.

The governing rules of confined concrete, proposed by Susantha, Ge and Usami (2002), are shown in Fig. 6. When unloading occur before peak point a, the unloading line have a slope of E_c. While, after peak point a, the unloading line make toward point b. Point b is decided by the intersection of vertical axis and the line originating from the peak point a, having a slop E_c. The tensile stress is ignored. Reloading is assumed to follow the same path as unloading in all the situations.

3.2 Effective concrete area

In the PCFST columns, concretes are not filled in the upper part of steel column. Therefore, the constitutive equation of PCFST column might be different from that of CFST column explained above. When we use the skeleton curve, as shown in Fig. 5, for numerical analysis of PCFST column, the strength will be overestimated.

It is assumed, in this model, that a separation between steel plate and concrete does not occur. However, experimental results showed that a separation occurred between steel plate and concrete especially when steel local buckling or elephant foot bulge occurred. And also there might be a slipping between steel plate and concrete. As a result, the strain in the cross-section is not continuous from steel plate to concrete. The strain of concrete at the surface should be lower than that of steel plates.

In this paper, to avoid the problems mentioned above, the cross-section of concrete is reduced by introducing a parameter. The effective concrete area is calculated by multiplication of the area of concrete and the parameter k_1. The parameter k_1 ($0 \leq k_1 \leq 1$) is determined from the following empirical equation;

$$k_1 = \begin{cases} (-169.6x^2 + 579.9x - 365.2)\left(\frac{L_c}{L}\right)^{1.3}\left(\frac{f_y}{f_c}\right)^{0.2}|\theta| \\ \qquad \text{(with diaphragm)} \\ (-247.1x^2 + 804.5x - 538.9)\left(\frac{L_c}{L}\right)^{1.3}\left(\frac{f_y}{f_c}\right)^{0.2}|\theta| \\ \qquad \text{(without diaphragm)} \end{cases} \tag{14}$$

with

$$\varepsilon_{cc} = \varepsilon_c\left\{1 + 5\left(\frac{f_{cc}}{f_c} - 1\right)\right\} \tag{15}$$

where θ is the slope angle of a base plastic-hinge region, $M_{z(s)}$ and $M_{z(s+c)}$ are the full plastic moment of a base plastic-hinge region without and with filled-in concrete, $M_{u(s+c)}$ is the ultimate moment of a base plastic-hinge region with filled-in concrete, respectively. The validity of parameter will be found in the numerical examples. In the calculations of full plastic moment $M_{z(s+c)}$ and $M_{u(s+c)}$, it is assumed that the tensile stress of concrete is ignored and the concrete is not subjected to the axial load. The ultimate moment $M_{u(s+c)}$ proposed by Iura, Orino and Ishizawa (2002) is employed. The stress and strain relationships of steel and concrete for $M_{u(s+c)}$ are shown in Fig. 7.

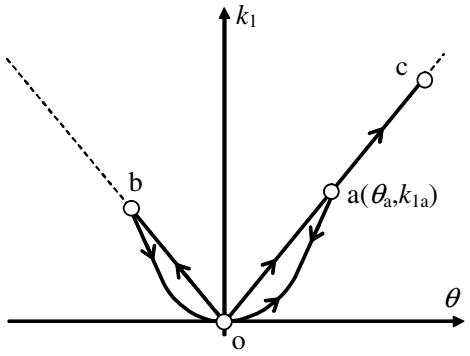

Figure 8 : Hysteretic rule of k_1.

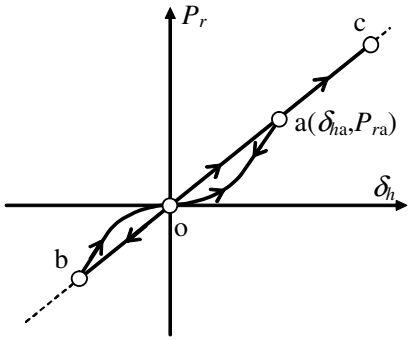

Figure 9 : Hysteretic rule of P_r.

A skeleton curve between parameter k_1 and slope angle θ is linear. A hysteretic rule of parameter $k_1$is defined on the basis of the fact that a starting point of the hardening delays after each cycle. A typical hysteretic curve of parameter k_1 is shown in Fig. 8. The thick solid line shows a hysteretic path o-a-o-b-o-a-c. At first it follows from o to a on the straight-line. When unloading occurs at point a(θ_a, k_{1a}), it follows on the quadratic-curve ao given by

$$k_1 = \frac{k_{1a}}{\theta_a^2}\theta^2 \tag{16}$$

When the slope angle θ reaches zero and becomes negative, it follows on the straight-line ob. When unloading occurs at point b, it follows the quadratic-curves bo and oa. After it reaches point a, it follows on the straight-line ac.

3.3 Model at second step

As mentioned earlier, a resisting force due to concretes in the elastic beam is obtained at second step. Let us consider a concrete cantilever beam with bending rigidity E_cI_c. The relation between tip load and tip displacement is well known. With the use of this equation, we define the resisting force P_r, expressed as

$$P_r = \frac{3E_cI_c}{L^3}\delta_h \times k_2 \tag{17}$$

with

$$k_2 = \begin{cases} 0.045\frac{L_c}{L} - 0.005 & \text{(with diaphragm)} \\ 0.045\frac{L_c}{L} & \text{(without diaphragm)} \end{cases} \tag{18}$$

where I_c is the moment of inertia of filled-in concrete, and the tip horizontal displacement δ_h is obtained in the first step. The parameter k_2 ($0 \leq k_2 \leq 0.045$) is introduced to express the hardening phenomena of PCFST columns.

A skeleton curve between the resisting force P_r and displacement δ_h is linear. A typical hysteretic curve is shown in Fig. 9. The thick solid line shows a hysteretic path o-a-o-b-o-a-c. At first it follows from o to a on the straight-line. When unloading occurs at point a(δ_{ha}, P_{ra}), it follows on the quadratic-curve ao, defined as

$$P_r = \frac{P_{ra}}{\delta_{ha}^2}\delta_h^2 \tag{19}$$

When the horizontal displacement δ_h reaches zero and becomes negative, it follows on the straight-line ob. When unloading occurs at point b, it follows on the quadratic-curves bo and oa. After it reaches point a, it follows on the straight-line ac.

4 Numerical results

At first step, the lateral load P_{h1} and the tip displacement δ_h are obtained with the use of the model, as shown in Fig. 2(b). Then the resisting force P_r is calculated by Eq. (17). Finally, the total resisting lateral force is obtained by addition of the lateral load P_{h1} and the resisting force P_r.

The validity of the present model has been confirmed through comparisons between experimental and numerical results. The dimensions and materials for test specimens are shown in Tab. 1, and the data for numerical analysis are shown in Tab. 2. The notation γ denotes the ratio of concrete and steel column height, defined as

$$\gamma = \frac{L_c}{L} \times 100(\%) \tag{20}$$

Table 1 : The dimensions and materials for test specimens.

	D mm	L mm	t mm	P_v kN	f_y MPa	f_m MPa	E_s GPa	υ	L_c mm	f_{ck} MPa	E_c GPa
No.1	502	1750	5.76	386	287	402	188	0.28	298	23.4	24.7
No.2	502	1750	5.76	386	287	402	188	0.28	490	24.4	25.2
No.3	502	1750	5.76	386	287	402	188	0.28	840	25.4	25.7
No.4	502	1750	5.94	375	270	402	195	0.29	998	36.3	29.9
No.5	400	1750	5.77	419	312	410	191	0.29	600	22.6	24.3
No.6	500	1750	5.76	335	313	437	195	0.28	998	37.1	30.1
No.7	400	1750	5.73	375	280	410	195	0.29	600	25.4	25.7

Table 2 : The various values for numerical analysis.

	γ %	$M_{z(s)}$ kN·m	$M_{z(s+c)}$ kN·m	$M_{u(s+c)}$ kN·m
No.1	17	396	492	585
No.2	28	396	500	594
No.3	48	396	509	603
No.4	57	384	578	697
No.5	34	272	240	355
No.6	57	428	625	732
No.7	34	243	236	345

Specimens No.1 to No.4 have no diaphragm, while specimens No.5 to No.7 have a diaphragm attached on the top of concrete.

4.1 Columns without diaphragm

The experimental results of Iura, Orino and Ishizawa (2002) are used for comparison. The test specimens have no diaphragm. The difference between these specimens is the ratio γ. Comparisons between experimental and numerical results are shown in Fig. 10. The dotted lines show the experimental results, while the solid lines the numerical results. The ratio γ is also shown in Fig. 10. In the experimental results, as the ratio γ become higher, the ultimate strength become higher. As shown in Fig. 10, the present numerical model was able to simulate the above phenomena with good accuracy. And good agreement between experimental and numerical results is obtained even after the ultimate strength.

4.2 Columns with diaphragm

Iura, Orino and Ishizawa (2002) have conducted an experimental work for PCFST column with a diaphragm. Comparisons between experimental and numerical results are shown in Fig. 11. These specimens have a diaphragm on the top of concrete. The ratio γ is also shown in Fig. 11. In the specimen No.7, the same displacement was repeated three times in each cycle. The agreement between experimental and numerical results is good. The hardening phenomena were captured by this model.

5 Discussions

We investigate the effects of two parameters introduced in this paper on the hysteretic curves. At first we put $k_1 = k_2 = 0$. The numerical result is shown in Fig. 12(a). This model corresponds to the steel columns without concrete. Therefore, numerical result underestimates the experimental results. The next model is made by putting $k_1 = 1$, $k_2 = 0$. It is assumed, in this model, that concretes in the base plastic-hinge region act without separation and slipping between steel plates and concretes. A comparison between experimental and numerical results is made in Fig. 12(b). As expected, the numerical result overestimates the experimental result. Finally we employ the parameter k_1 defined by Eqs.(14) and (16), and put $k_2 = 0$. This model neglects the effect of concretes in the elastic beam on mechanical behavior of PCFST column. A comparison between experimental and numerical result is shown in Fig. 12(c). Good agreement was obtained in this case. However, a comparison between Fig. 10(b) and 12(c) indicates that the inclusion of parameter k_2 yields to much better accuracy for numerical analysis.

6 Conclusions

A one-dimensional model has been proposed for the analysis of circular PCFST columns. The main issue of analysis of PCFST columns subjected to cyclic loadings is to simulate the hardening phenomena after a few cycles. The idea of the present method is to introduce

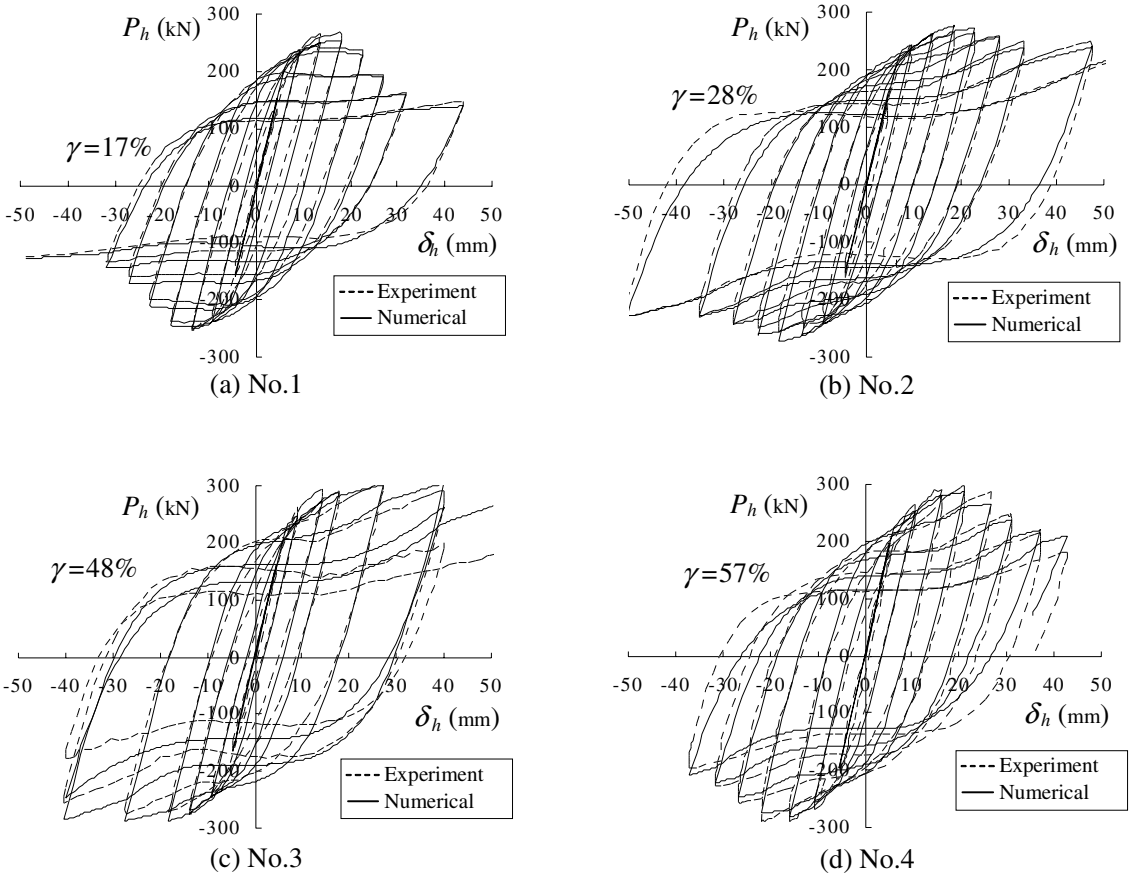

Figure 10 : Hysteretic curves: These specimens have no diaphragm.

the parameters k_1 and k_2 in order to obtain the hardening phenomena. The advantage of the present model is that experiments or shell analysis are not required to establish a constitutive equation of steel plate and filled-in concrete. The constitutive equation of steel plate, which is obtained by Ishizawa and Iura (2005), was employed in present model. Moreover, the effective concrete area and the resisting force are introduced in order to express the hardening phenomena of PCFST columns subjected to cyclic loading. Comparisons of experimental and numerical results showed good agreement.

References

Amano, M.; Kasai, A.; Usami, T.; Ge, H.; Okamoto, S; Maeno, H. (1998): Experimental and analytical study on elasto-plastic behavior of partially concrete-filled steel piers. *Journal of Structural Engineering, JSCE*, vol.44A, pp. 179-188.

Chu, K.; Sakurai, T. (2004): Reinforcement method for improvement of earthquake-proof capacity on existing cylindrical steel piers by welded steel plates. *The 2nd International Conference on Steel & Composite Structures*, Seoul, Korea, September 2-4.

Ferretti, E. (2004): Crack-path analysis for brittle and non-brittle cracks: A cell method Approach. *CMES: Computer Modeling in Engineering and Sciences*, vol. 6, No.3, pp. 227-244.

Ge, H.; Usami, T. (1996): Cyclic tests of concrete-filled steel box columns. *Journal of Structural Engineering, ASCE*, 122(10), pp. 1169-1177.

Iura, M.; Kumagai, Y.; Komaki, O. (1997): Ultimate strength of stiffened cylindrical shells subjected to axial and lateral forces. *Journal of Structural Mechanics and Earthquake Engineering*, *JSCE*, No.556/I-38, 107-118.

Iura, M.; Orino, A.; Ishizawa, T. (2002): Elasto-plastic behavior of concrete-filled steel tubular columns. *Jour-*

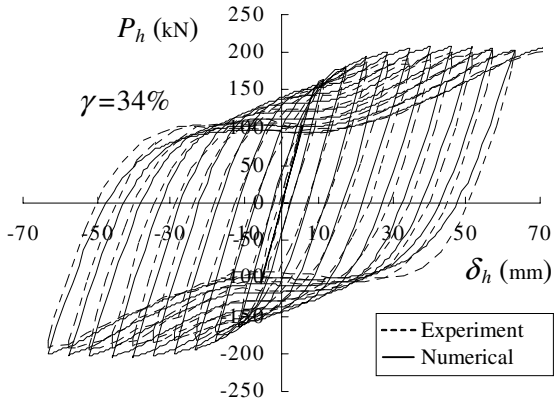

(a) No.5

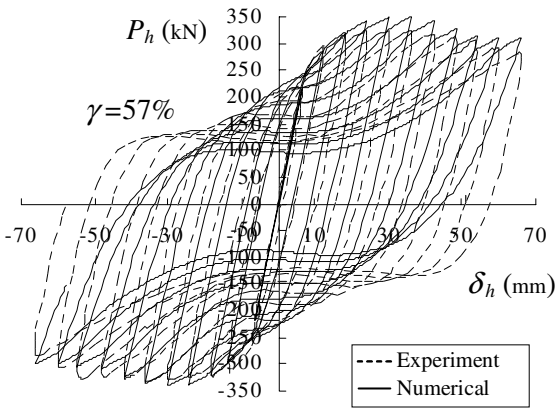

(b) No.6

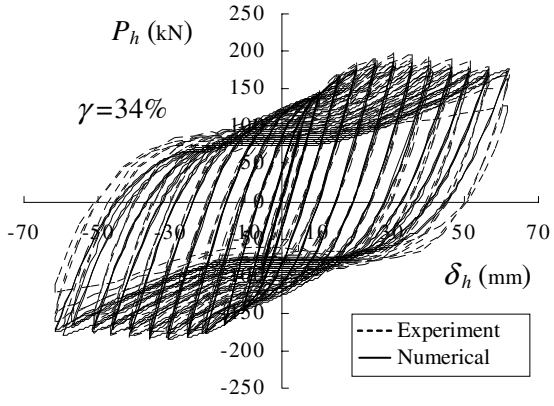

(c) No.7

Figure 11 : Hysteretic curves: These specimens have a diaphragm.

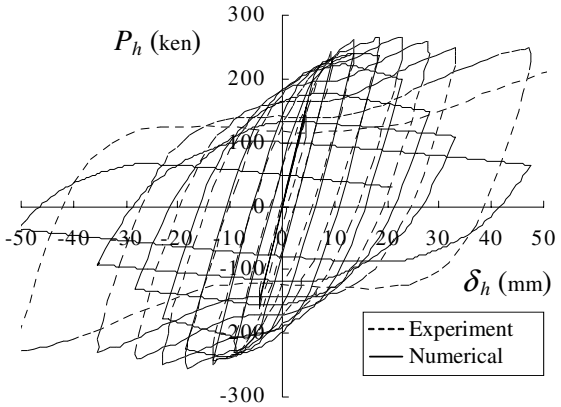

(a) k_1=k_2=0

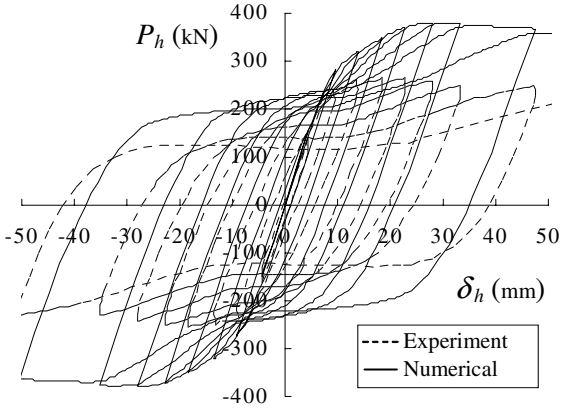

(b) k_1=1, k_2=0

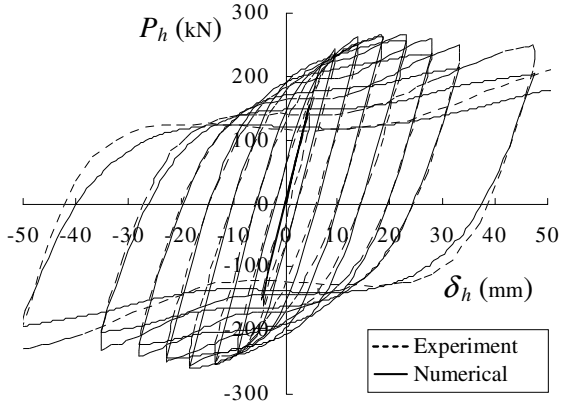

(c) k_1 is defined by Eqs. (14) and (16), k_2=0

Figure 12 : Hysteretic curves for No.2.

nal of Structural Mechanics and Earthquake Engineering, *JSCE*, No.696/I-58, pp. 285-298.

Iura, M.; Suetake, Y.; Atluri, S.N. (2003): Accuracy of Co-rotational formulation for 3-D Timoshenko's beam. *CMES: Computer Modeling in Engineering and Sciences*, vol. 4, No.2, pp. 249-258.

Ishizawa, T.; Iura, M. (2005): Analysis of tubular steel piers. *Earthquake Engineering and Structural Engineering*, 34, pp. 985-1004.

Morishita, M.; Aoki, T.; Suzuki M. (2000): Experimental study on the seismic resistance performance of concrete-filled steel tubular columns. *Journal of Structural Engineering*, *JSCE*, Vol.46A, pp.73-83.

Public Works Research Institute; Metropolitan Expressway Public Corp.; Hanshin Expressway Public Corp.; Nagoya Expressway Public Corp.; Kozai Club,; Japan Association of Steel Bridge Construction (1997): Joint Research Report on Limit State Seismic Design of highway Bridge Piers (I-VII).

Sakai, J.; Kawashima, K. (2003): Modification of the Giuffre, Menegotto and Pinto model for unloading and reloading paths with small strain variations. *Journal of Structural Mechanics and Earthquake Engineering*, *JSCE*, No.738/I-64, pp. 159-169.

Susantha, K. A. S.; Ge, H.; Usami, T. (2001): Uniaxial stress-strain relationship of concrete confined by various shaped steel tubes. *Engineering Structure*, 23, pp. 1331-1347.

Susantha, K. A. S.; Ge, H.; Usami, T. (2002): Cyclic analysis and capacity prediction of concrete-filled steel box columns. *Earthquake Engineering and Structural Engineering*, 31, pp. 195-216.

Tang, J.; Hino, S.; Kuroda, I.; Ohta, T. (1996): Modeling of stress-strain relationships for steel and concrete in concrete filled circular steel tubular columns. *Steel Construction Engineering*, *JSSC*, 3(11), pp. 35-46.

Usami, T.; Ge, H. (1994): Ductility of concrete-filled steel box columns under cyclic loading. *Journal of Structural Engineering*, *ASCE*, 120(7), pp. 2021-2040.

Watanabe, T.; Ishida, K.; Hayashi, K.; Yamaguchi, T.; Ikeda, S. (2002): Seismic retrofit of steel piers with carbon fiber sheets. *Journal of Structural Engineering*, *JSCE*, Vol.48A, pp. 725-734.